UNIVERSITY OF COPENHAGEN

Trends in CO2 exchange in a high Arctic tundra heath, 2000-2010

Lund, Magnus; Falk, Julie Maria; Friborg, Thomas; Mbufong, Herbert N.; Sigsgaard, Charlotte; Søgaard, Henrik; Tamstorf, Mikkel P.

Published in:
Journal of Geophysical Research

Publication date:
2012

Document version
Peer reviewed version

Citation for published version (APA):
Lund, M., Falk, J. M., Friborg, T., Mbufong, H. N., Sigsgaard, C., Søgaard, H., & Tamstorf, M. P. (2012). Trends in CO_2 exchange in a high Arctic tundra heath, 2000-2010. *Journal of Geophysical Research*, *117*(G2).

Download date: 19. sep.. 2020

Trends in CO_2 exchange in a high Arctic tundra heath, 2000–2010

Magnus Lund,[1] Julie M. Falk,[2] Thomas Friborg,[3] Herbert N. Mbufong,[1] Charlotte Sigsgaard,[1,3] Henrik Soegaard,[3] and Mikkel P. Tamstorf[1]

Received 28 October 2011; revised 7 February 2012; accepted 12 February 2012; published 4 April 2012.

[1] We have measured the land-atmosphere CO_2 exchange using the eddy covariance technique in a high Arctic tundra heath in northeast Greenland (Zackenberg). On the basis of 11 years of measurements (2000–2010), it was found that snow cover dynamics was important for the CO_2 exchange. The start of CO_2 uptake period correlated significantly with timing of snowmelt. Furthermore, for years with deep and long-lasting snowpacks, the following springs showed increased CO_2 emission rates. In the first part of the study period, there was an increase of approximately 8 g C m^{-2} yr^{-1} in both accumulated gross primary production (GPP) and CO_2 sink strength during summer. However, in the last few years, there were no significant changes in GPP, whereas ecosystem respiration (R_{eco}) increased (8.5 g C m^{-2} yr^{-1}) and ecosystem CO_2 sink strength weakened (−4.1 g C m^{-2} yr^{-1}). It was found that temperature and temperature-related variables (maximum thaw depth and growing degree days) controlled the interannual variation in CO_2 exchange. However, while R_{eco} showed a steady increase with temperature (5.8 g C m^{-2} °C^{-1}), the initial increase in GPP with temperature leveled off at the high end of observed temperature range. This suggests that future increases in temperature will weaken the ecosystem CO_2 sink strength or even turn it into a CO_2 source, depending on possible changes in vegetation structure and functioning as a response to a changing climate. If this trend is applicable also to other Arctic ecosystems, it will have implications for our current understanding of Arctic ecosystems dynamics.

Citation: Lund, M., J. M. Falk, T. Friborg, H. N. Mbufong, C. Sigsgaard, H. Soegaard, and M. P. Tamstorf (2012), Trends in CO_2 exchange in a high Arctic tundra heath, 2000–2010, *J. Geophys. Res.*, *117*, G02001, doi:10.1029/2011JG001901.

1. Introduction

[2] During recent decades the observed warming in the Arctic has been almost twice as large as the global average [*Graversen et al.*, 2008]. Increasing temperatures and changes in precipitation patterns will affect most components of the Arctic environment, including permafrost, hydrology, vegetation and carbon (C) and nutrient cycling. Northern high-latitude terrestrial ecosystems contain large stocks of soil organic C; these stocks are the result of net C accumulation during thousands of years promoted by cold and poorly aerated soil conditions inhibiting decomposition rates. A recent estimate of the soil C storage in northern high-latitude terrestrial ecosystems is 1400 to 1850 Pg C [*McGuire et al.*, 2009]. The effects of a changing climate will result in significant and important changes on the exchanges of carbon dioxide (CO_2) and methane (CH_4), which are likely to pose a strong feedback effect on global warming [*Schuur et al.*, 2008; *Tarnocai et al.*, 2009; *McGuire et al.*, 2010].

[3] Recent observations from circumpolar permafrost monitoring sites reveal that permafrost temperatures have increased [*Romanovsky et al.*, 2010]. In a climate-manipulation experiment in a subarctic peatland [*Dorrepaal et al.*, 2009], an increase of 1°C in air and soil temperatures caused a large increase in ecosystem respiration (R_{eco}), and a majority of the increase originated from old C in subsurface peat. An increase in vegetation greenness and productivity has been observed in northern high-latitude terrestrial ecosystems, mainly associated with an expansion of shrubs [*Sturm et al.*, 2001; *Tape et al.*, 2006]. Through measurements of the net ecosystem exchange (NEE) of CO_2 in a tundra landscape undergoing permafrost thaw, *Schuur et al.* [2009] found that after approximately 15 years of permafrost thaw the loss of old C began to offset increased C uptake by plants through gross primary production (GPP), turning the tundra ecosystem into a C source. Thawing permafrost and increased deepening of the active layer will also have profound effects on water tables, soil moisture and redox state. In well-drained areas, drought conditions can become more prevalent as the active layer depth increases, stimulating CO_2 emissions by enhanced soil aeration [*Oechel et al.*, 1993]. By contrast, some areas will become wetter favoring anaerobic C mineralization and CH_4 production [*Johansson et al.*, 2006]. Climate warming induced increases in soil mineralization rates will also increase nutrient availability [*Rustad et al.*, 2001],

[1]Department of Bioscience, Aarhus University, Roskilde, Denmark.
[2]Department of Earth and Ecosystem Sciences, Lund University, Lund, Sweden.
[3]Department of Geography and Geology, University of Copenhagen, Copenhagen, Denmark.

Copyright 2012 by the American Geophysical Union.
0148-0227/12/2011JG001901

affecting vegetation properties and composition and soil C storage [*Mack et al.*, 2004; *Malmer and Wallén*, 2005].

[4] The land-atmosphere CO_2 exchange in tundra ecosystems is primarily controlled by the short growing season exchange. However, losses during shoulder seasons and winter period are also of importance [*Nordstroem et al.*, 2001; *Johansson et al.*, 2006; *Wang et al.*, 2011]. Interannual variation in NEE has been found to be related to air temperature and date of snowmelt, as the snow-free period regulates the temporal borders for potential photosynthetic C assimilation [*Aurela et al.*, 2004; *Grøndahl et al.*, 2007]. Soil wetness is also an important factor as drier conditions may increase decomposition rates and decrease GPP [*Oechel et al.*, 1993; *Aurela et al.*, 2007; *Lund et al.*, 2007].

[5] During the past decades, the eddy covariance (EC) method has become a key tool for measuring CO_2 exchange at landscape level. An advantage with EC measurements compared with leaf cuvettes and soil chambers is that it allows landscape monitoring of whole ecosystem CO_2 exchange, which makes it especially appropriate for studying ecosystem C balance and physiology [*Baldocchi*, 2003]. Compared with lower latitudes, Arctic sites are underrepresented in EC flux networks such as Fluxnet [*Baldocchi et al.*, 2001]. The harsh conditions and remoteness of the Arctic make measurements difficult, especially during wintertime. However, owing to instrumental improvements and increased awareness of the importance of the Arctic in terms of greenhouse gas exchange, more and more EC CO_2 flux data are now becoming available from this vast area [*Soegaard and Nordstroem*, 1999; *Vourlitis and Oechel*, 1999; *Vourlitis et al.*, 2000; *Lloyd*, 2001; *Nordstroem et al.*, 2001; *Harazono et al.*, 2003; *McFadden et al.*, 2003; *Aurela et al.*, 2004; *Corradi et al.*, 2005; *Johansson et al.*, 2006; *Lafleur and Humphreys*, 2008; *Grøndahl et al.*, 2007, 2008; *Kutzbach et al.*, 2007; *Humphreys and Lafleur*, 2011; *Parmentier et al.*, 2011].

[6] The main objective of this study is to investigate the effects of the strong climate warming observed during the last decade in the high Arctic on the CO_2 dynamics in a northeast Greenlandic tundra heath. We hypothesize that climate warming has increased both GPP and R_{eco}, and that the initial net effect of the opposing flux components will be of increased C sink strength, that is, higher net CO_2 uptake. A possible increase in ecosystem CO_2-C accumulation is likely to be temporary as the active layers become thicker allowing for increased decomposition rates, in accordance with *Schuur et al.* [2009]; however, the time scale of a possible sink-to-source transition should be site specific.

[7] Based on 11 years (2000–2010) of eddy covariance measurements of land-atmosphere CO_2 exchange from a high Arctic tundra heath site in northeast Greenland (Zackenberg), this paper describes interannual variation in NEE and its components (GPP and R_{eco}). It is found that R_{eco} shows a steady increase with temperature, whereas the increase in GPP levels off at the high end of observed temperature range.

2. Materials and Methods

2.1. Site Description

[8] The CO_2 flux measurements were conducted in the Zackenberg valley within the Northeast Greenland National Park (74.47°N, 20.55°W, elevation: 38 m). This area has been subjected to extensive environmental research activities during the last 15 years within the auspices of Zackenberg Ecological Research Operations (ZERO). The annual mean (1996–2010) temperature is −9.0°C with July as the warmest month (6.2°C) and February as the coldest (−22.4°C). Annual precipitation sum is 261 mm, of which approximately 85% falls as snow [*Hansen et al.*, 2008]. The area is underlain by permafrost; and the maximum thaw depth is ca. 0.8 m in late summer. During 1996–2009 the mean annual temperature has increased by 0.15°C yr^{-1}; with the highest increase occurring in July (0.27°C yr^{-1}) [*Jensen and Rasch*, 2010]. At the same time, the maximum thaw depth has increased by 1.4–1.8 cm yr^{-1}. Winds during winter are typically from north, while during summer southeasterly winds dominate [*Hansen et al.*, 2008]. The soils are slightly acidic; ranging pH 5–5.5 in the top 20 cm [*Elberling et al.*, 2008]. The eddy covariance (EC) system was installed in a tundra heath (Figure 1), which is the dominating ecosystem type in the area. Vegetation within the fetch is dominated by *Cassiope tetragona*, *Dryas integrifolia* and *Vaccinium uliginosum*, accompanied by patches of mosses, *Salix arctica* and *Eriophorum scheuchzeri.* Summertime soil water content in the topsoil at the study site is approximately 30% while maximum leaf area index (LAI) generally ranges 0.2–0.3.

2.2. Measurements

[9] The flux measurements in 2000–2010 were conducted during the time period each year when the Zackenberg Research Station was manned. This time period generally spanned from early June until late August in the early years; while it has been extended to early May until late October in the last few years (differences in measurement time period have been accounted for, see section 2.4). Between 2000 and late 2007 the EC system consisted of an infrared gas analyzer LI-6262 (LI-COR Inc, USA) and a 3D sonic anemometer Gill R2 (Gill Instruments Ltd, UK). Since late 2007, a LI-7000 (LI-COR Inc, USA) and a Gill R3 (Gill Instruments Ltd, UK) have been used. The anemometer was installed at a height of 3 m, and air was drawn at a rate of ∼5.2 L min^{-1} through 7 m of tubing, equipped with a 1 μm pore size filter (Gelman Acro 50), to the gas analyzer. Soda lime and magnesium perchlorate were used to scrub the reference cell from CO_2 and H_2O, respectively. The offset and span of the gas analyzers were checked regularly. In all directions surrounding the mast, there are at least 300 m with homogeneous surface properties. More information on the EC system is given by *Moncrieff et al.* [1997], *Soegaard et al.* [2000], and *Grøndahl et al.* [2007].

[10] Approximately 150 m from the EC mast (Figure 1), a meteorological station operated by Asiaq–Greenland Survey provides a wide range of quality checked ancillary data, including air temperature and humidity (Vaisala, HMP 45D), precipitation (Ott Pluvio and Belfort, 5915 x), snow depth (Campbell, SR50–45), photosynthetic photon flux density (PPFD; LI-COR, LI-190SA) and surface and soil temperatures at depths 2.5, 5, 10, 20, 30, 40 and 60 cm (Campbell, 105T). In addition, active layer depth was measured in a nearby active layer monitoring area, ZERO-CALM (Circumpolar Active Layer Monitoring-Network-II), in biweekly intervals.

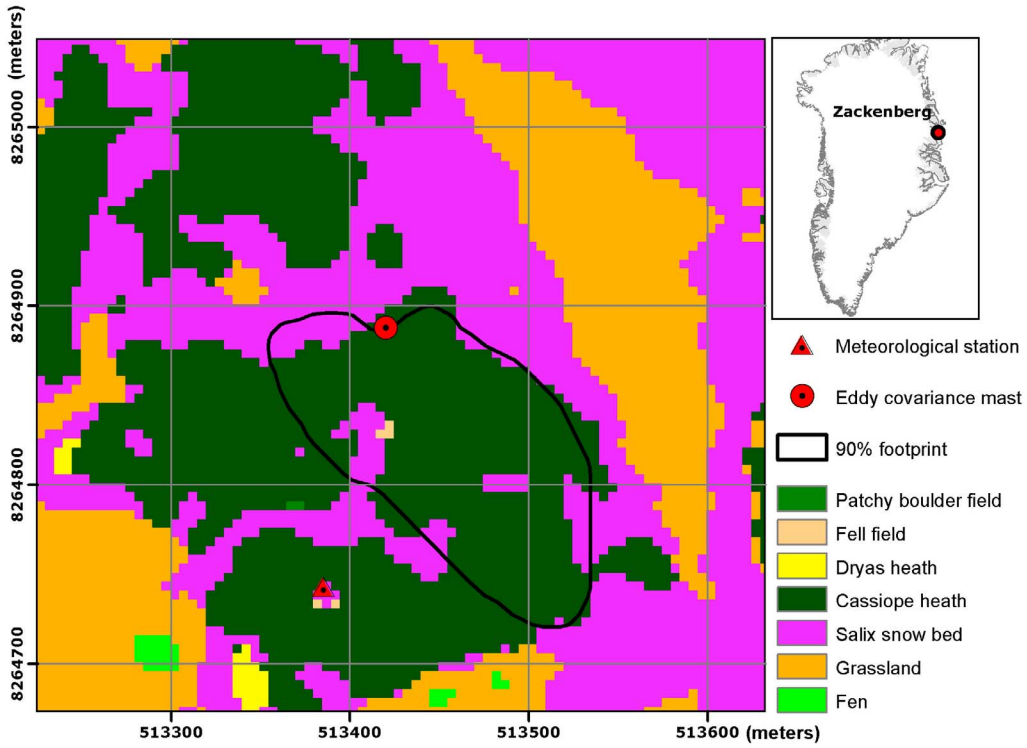

Figure 1. Map of plant community classes (defined in *Elberling et al.* [2008]) in the vicinity of eddy covariance mast in Zackenberg, northeast Greenland (Universal Transverse Mercator (UTM) zone 27, World Geodetic System (WGS) 84). Solid black line depicts the mean 90% footprint of the eddy covariance system calculated for 9 June to 24 August 2010. Inset map shows the location of Zackenberg in northeast Greenland (74.47°N, 20.55°W, elevation: 38 m).

2.3. Data Handling

[11] Data from the eddy covariance system were acquired from the analyzers' digital-to-analogue converters, aligned to anemometer data, and collected on a computer running Edisol software [*Moncrieff et al.*, 1997]. Raw data files were processed in EdiRe software (Robert Clement, University of Edinburgh) and fluxes calculated on a 30 min basis. The processing list includes despiking [*Højstrup*, 1993], 2-D coordinate rotation, time lag removal between anemometer and gas analyzer data by optimizing covariance, block averaging, frequency response corrections based on model spectra and transfer functions [*Moore*, 1986], and WPL correction [*Webb et al.*, 1980]. The instrumental error of the combined CO_2 flux system has been estimated to ±7% [*Soegaard et al.*, 2000]. Postprocessing in Matlab R2010a (The Mathworks, Inc., USA) includes storage term calculation based on the single point gas analyzer CO_2 concentration measurements, and flux screening for periods with low friction velocity ($u_* < 0.1$ m s^{-1}; 38% of data set).

[12] Gaps in CO_2 flux data were filled using three approaches. First, gaps smaller than 2 hours were filled using linear interpolation. Second, the *Misterlich* function [*Falge et al.*, 2001] was parameterized for daytime periods (PPFD > 10 μmol m^{-2} s^{-1}) using an 8 day moving window (time step 1 day) with PPFD as an independent variable:

$$NEE = -(F_{csat} + R_d)(1 - e^{\frac{-\alpha(PPFD)}{F_{csat}+R_d}}) + R_d, \quad (1)$$

where F_{csat} is CO_2 uptake rate at light saturation, R_d is dark respiration, and α is initial slope of light response curve. The parameterization of the light response curve was only considered significant when all parameters (F_{csat}, R_d, α) were significantly different from zero ($p < 0.05$). Remaining gaps were filled with mean diurnal variation using an 8 day window [*Falge et al.*, 2001]. To evaluate the performance of these gap-filling procedures we compared gap-filled data from the measuring period in 2002 (3 June to 22 August, 44% gaps) with the online gap-filling tool (http://www.bgc-jena.mpg.de/bgc-mdi/html/eddyproc), which is similar to the gap-filling procedures used, for example, in Fluxnet [*Baldocchi et al.*, 2001]. The difference in accumulated CO_2-C was 1.2 g C m^{-2}; the gap-filling procedures used in this study resulted in a sink of −6.1 g C m^{-2}, while using the online gap-filling tool the sink was estimated to be −4.8 g C m^{-2}. The reason for not using the online gap-filling tool or similar methodologies was that the light response curve method enabled flux partitioning into gross primary production (GPP) and ecosystem respiration (R_{eco}, see section 2.4), without being dependent on nighttime conditions; as the high-latitude location of the Zackenberg area has midnight sun between 30 April and 12 August.

2.4. Data Analyses

[13] In order to investigate the interannual variation in accumulated NEE for years with measurement periods of varying lengths, the time period for which data were available for all 11 years (2000–2010) was chosen, namely, day

of year (DOY) 160–236 (9 June to 24 August for non leap years). Gross primary production was modeled using the light response curves (equation (1)) by subtracting R_d [*Lindroth et al.*, 2007]. Daytime (PPFD > 10 μmol m^{-2} s^{-1}) R_{eco} was calculated as the difference between measured and gap-filled NEE and modeled GPP; while nighttime (PPFD ≤ 10 μmol m^{-2} s^{-1}) R_{eco} equaled measured and gap-filled NEE. Since the light response curve parameterization (equation (1)) were considered significant for different time periods in each year, the accumulated GPP and R_{eco} were consequently calculated for those different time periods in each year.

[14] The interannual variation in accumulated NEE, GPP and R_{eco} were analyzed for linear correlation with the following environmental variables: air temperature (AirT); growing degree days (GDD) with base temperature 0°C [*Jensen and Rasch*, 2010]; photosynthetic photon flux density (PPFD); precipitation (Precip); DOY of snowmelt (DOY when snow cover < 0.1 m; SM DOY); maximum thaw depth (max. Thaw); and normalized difference vegetation index (NDVI). The NDVI data were obtained from Earth observation data using SPOT, Landsat TM and ETM+ and ASTER products from around 1 August each year (±one week), calculated as the average for each pixel (15 m to 30 m pixel resolution depending on sensor) that was included by more than 50% by the average flux footprint (see section 2.6 and Figure 1). All variables were tested for normality using a two-sided goodness-of-fit Lilliefors test (Matlab R2010a, The Mathworks, Inc., USA); variables rejecting the null hypothesis that the sample comes from a normal distribution were transformed to normality.

2.5. Uncertainty Assessment

[15] Estimates of flux uncertainties are important for proper interpretation of interannual variation and long-term trends in eddy covariance flux measurements [*Elbers et al.*, 2011]. The random error uncertainty (E_{rand}) associated with measurement and CO_2 flux calculation was calculated from the difference between observed and modeled half hourly NEE fluxes according to *Aurela et al.* [2002]. Systematic errors can arise from insufficient coverage of the high-frequency contribution to turbulent fluxes, due to limited sensor response time, tube attenuation and sensor separation. Such losses were systematically accounted for (see section 2.3), and the frequency response correction for CO_2 flux was on average 19%. Similar to *Aurela et al.* [2002], we assume an uncertainty of 30% for the frequency response correction (E_{freq}) in each year. The selection of u_* threshold, below which measured CO_2 fluxes were discarded and replaced by modeled fluxes based on periods with sufficiently developed turbulence, may introduce additional uncertainty. This was assessed by evaluating the effect of using a deviation of ±0.05 m s^{-1} around the default u_* threshold (0.1 m s^{-1} in this study) on the seasonal CO_2 sum [*Elbers et al.*, 2011]. The uncertainty (E_{ustar}) was determined from the standard deviation of the three NEE sums (u_* thresholds of 0.05, 0.10 and 0.15 m s^{-1}, respectively). Finally, the uncertainty related to gap filling was assessed by reversing the gap distribution of one randomly selected year (year 2001) and apply it to all other years, and repeating the gap-filling procedure for the artificial gaps. The standard deviation of the two seasonal sums based on original data and data with artificial gaps were used to represent E_{gap}. The total uncertainty for seasonal sums of NEE (E_{NEE}) was calculated using the error accumulation principle:

$$E_{NEE} = \sqrt{E_{rand}^2 + E_{freq}^2 + E_{ustar}^2 + E_{gap}^2}. \quad (2)$$

For seasonal sums of GPP, which was modeled on the basis of light response curves (equation (1)), the uncertainty was based on E_{rand}, E_{freq} and E_{ustar}; as well as the uncertainty associated with parameterizing the light response curve. This uncertainty (E_{LRC}) was assessed by recalculating the GPP sum for each year using ±1 standard deviation for each parameter (F_{csat}, R_d, α). The total uncertainty for seasonal sums of GPP (E_{GPP}) was thus calculated as

$$E_{GPP} = \sqrt{E_{rand}^2 + E_{freq}^2 + E_{ustar}^2 + E_{LRC}^2}. \quad (3)$$

Daytime (PPFD > 10 μmol m^{-2} s^{-1}) R_{eco} rates were calculated as the difference between measured and gap-filled NEE and GPP, while nighttime R_{eco} rates equaled NEE rates. The uncertainty in seasonal sums of R_{eco} (E_{Reco}) was therefore calculated as

$$E_{R_{eco}} = a\sqrt{E_{NEE}^2 + E_{GPP}^2} + bE_{NEE}, \quad (4)$$

where a and b are the fractions of daytime and nighttime half hours, respectively, to the total number of half hours during the time periods in each year for which R_{eco} was accumulated.

2.6. Footprint Analysis

[16] We have used the *Schuepp et al.* [1990] footprint model, adapted to a GIS environment [*Soegaard et al.*, 2003]. The purposes of the footprint modeling were to investigate whether other ecosystems except for the heath ecosystem would have impact on the measured fluxes, and to select proper pixels for NDVI calculations. A threshold of 90% was used for the spatial extent of the footprint. Only data with sufficient atmospheric mixing (u_* > 0.1 m s^{-1}) were used in the calculations, as only such data were included in the other analyses. The flux footprint was calculated for the period 9 June to 24 August 2010, which is the same time period as NEE was accumulated. Wind direction characteristics for the Zackenberg area during summer are stable from year to year [*Hansen et al.*, 2008], and on the basis of the sonic anemometer data, the most common 30° wind direction bin was 120°–150° in all years except for 2008 (150°–180°). The flux footprint of 2010 was therefore considered as representative also for earlier measurement years.

3. Results

[17] The footprint modeling (Figure 1) indicated that a majority of the detected CO_2 fluxes emanated from the *Cassiope* heath plant community type. The *Cassiope* heath is the dominating plant community type in all directions surrounding the eddy covariance system except for the 0°–90° sector, where *Salix* snow bed and grassland plant community types are dominating. The proportion of accepted (non gap-filled) fluxes between 9 June and 24 August (see

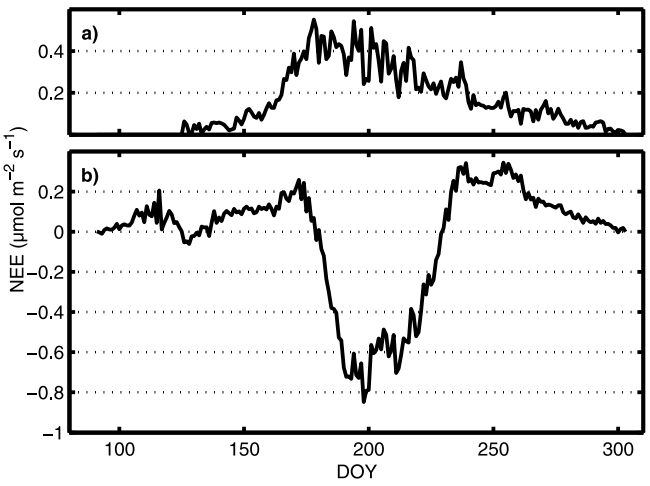

Figure 2. Average year (2000–2010) net ecosystem exchange (NEE) in a high Arctic heath in Zackenberg, northeast Greenland. (a) Standard deviation in mean daily NEE between individual years. (b) Mean daily measured and gap-filled NEE.

section 2) originating from this sector averaged 6.9 ± 2.3% during the study period (range: 4.1% in 2007 to 10.1% in 2005). However, since the Zackenberg valley is a composite of various plant communities and sub ecosystems, we consider our entire data set as a representative indicator of NEE in a drier part of the Zackenberg tundra, where the *Cassiope* heath plant community type is dominating.

[18] The temporal variation in mean daily net ecosystem exchange of CO_2 (NEE) for an average year (2000–2010) in the Zackenberg tundra heath is shown in Figure 2. The sign convention used in all figures and tables in this paper is the standard one for micrometeorological measurements; fluxes directed from surface to atmosphere (emissions) are positive, while fluxes directed from atmosphere to surface (uptake) are negative. During early spring and late autumn, when temperatures remain below freezing, daily average fluxes were low (<0.1 μmol m^{-2} s^{-1}). In late spring and early autumn, just before and after the period of mean daily net CO_2 uptake, highest mean daily CO_2 fluxes were detected (>0.2 μmol m^{-2} s^{-1}). On average, the heath switched from being a source of CO_2 to a sink on a daily basis on DOY 177 (26 June for non leap years), and remained so until DOY 229 (17 August; Table 1). The timing of start of mean daily net CO_2 uptake period, which correlated significantly with DOY of snowmelt ($p = 0.001$), was more variable (SD = 10.3) compared with timing of end of net uptake period (SD = 2.9). Maximum mean daily net CO_2 uptake occurred on average on DOY 197 (16 July; SD = 8.9) with an average rate of −1.1 ± 0.1 μmol m^{-2} s^{-1} (mean ± SD; Table 1).

[19] In some years, namely, 2001–2004, 2008 and 2010 (hereinafter referred to as the spring CO_2 burst years), CO_2 emissions were greater compared with other years in the period between snowmelt (mean DOY when snow cover <0.1 m = 165; 14 June) and start of net uptake period (Figure 3). On average, accumulated NEE between snowmelt and start of net uptake period was significantly different ($t = 5.5$; $p < 0.001$) for spring CO_2 burst years (6.1 ± 1.3 g C m^{-2}) as compared with other years (1.3 ± 1.6 g C m^{-2}). For

Table 1. Summary of the CO_2 Flux Measurement Periods, Maximum Net Uptake Rates, and Accumulated NEE, GPP, and R_{eco} With Associated Uncertainty Estimates

	2000	2001	2002	2003	2004	2005	2006	2007	2008	2009	2010
Measurements start (DOY)	158	159	154	157	155	141	148	147	90	136	125
Measurements end (DOY)	238	238	239	242	241	237	239	301	302	295	304
Start of net uptake period (DOY)	177	188	183	180	175	159	189	167	188	164	182
End of net uptake period (DOY)	226	229	228	227	229	228	235	231	233	227	226
Measuring period NEE (g C m^{-2})	−18.8	−2.1	−5.4	−13.8	−13.2	−37.9	−24.9	−28.2	−11.2	−11.0	5.0
Similar period NEE (g C m^{-2})[a]	−19.4 ± 2.6	−4.3 ± 2.6	−5.9 ± 1.4	−15.6 ± 1.8	−16.2 ± 1.4	−39.7 ± 3.1	−25.8 ± 1.6	−37 ± 2.6	−24.9 ± 1.6	−21.9 ± 1.7	−16.0 ± 2.3
Maximum daily net uptake rate (μmol m^{-2} s^{-1})	−1.06	−1.06	−0.86	−1.22	−1.10	−1.35	−1.07	−1.27	−1.26	−0.93	−1.10
Maximum daily net uptake rate (DOY)	190	195	191	192	199	194	213	190	216	195	196
GPP (g C m^{-2})[b]	−59.7 ± 8.5	−54.1 ± 7.7	−67.7 ± 7.6	−92.3 ± 10.2	−82.7 ± 9.2	−95.4 ± 10.7	−68.4 ± 8.6	−86.3 ± 11.8	−87.9 ± 11.9	−85.4 ± 10.4	−84.2 ± 8.8
R_{eco} (g C m^{-2})[b]	37.9 ± 8.7	37.7 ± 8.0	52.1 ± 7.3	67.7 ± 9.9	58.9 ± 8.9	56 ± 10.7	39.8 ± 8.3	48.7 ± 11.9	61.4 ± 10.8	63.8 ± 10.2	58.7 ± 9.0

[a]Net ecosystem exchange (NEE) was accumulated for the period DOY 160–236 in each year.
[b]Gross primary production (GPP) and ecosystem respiration (R_{eco}) were accumulated for the period in each year when the parameterization of the light response curves (equation (1)) was considered significant.

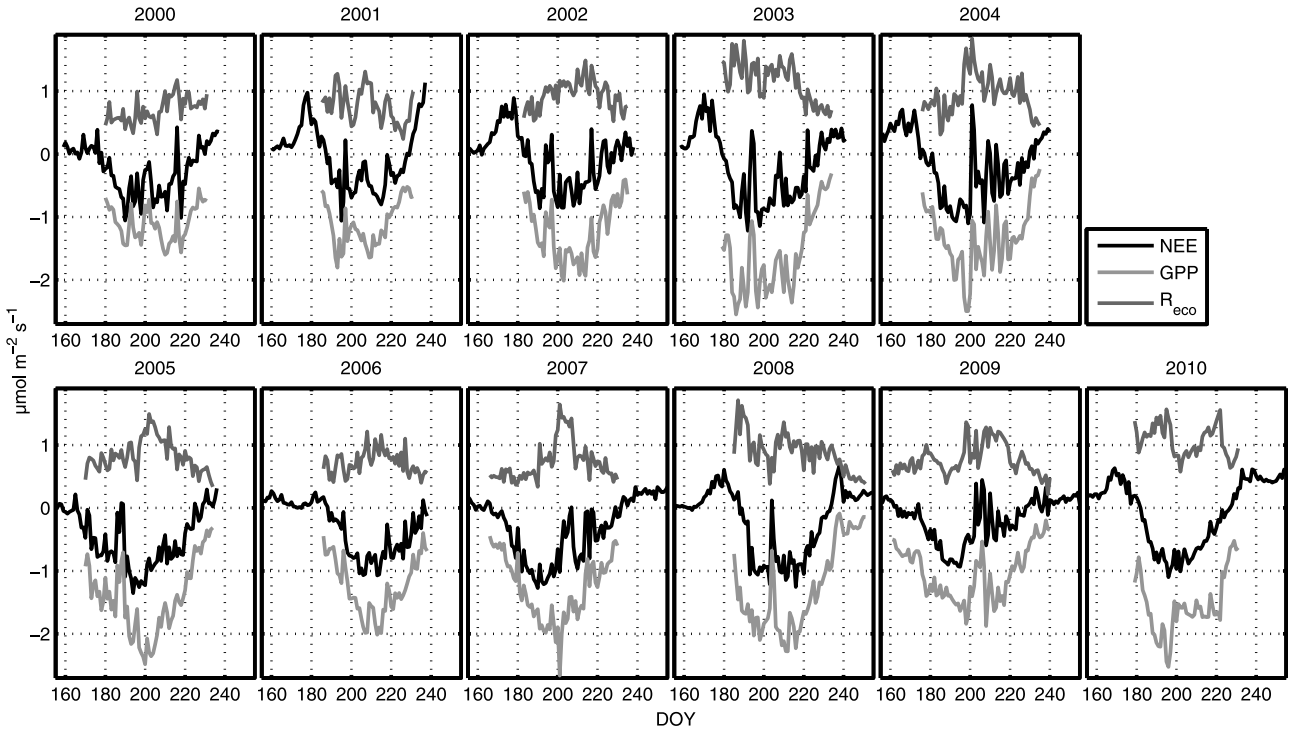

Figure 3. Time series of CO_2 flux components from a high Arctic heath in Zackenberg, northeast Greenland. Solid black lines depict mean daily measured and gap-filled NEE, solid light gray lines depict modeled gross primary production (GPP), and solid dark gray lines depict modeled ecosystem respiration (R_{eco}).

the same period of time in each year, there was a significant difference in mean surface temperature (t = 2.3; p = 0.043) between spring CO_2 burst years (8.8 ± 1.0°C) and other years (5.6 ± 3.2°C). The years with higher surface temperatures generally had a deep and long-lasting snowpack during preceding winter period. The duration of the snowpack was significantly different (t = 2.6, p = 0.030) in spring CO_2 burst years (219 ± 30 days) compared with other years (167 ± 38 days). Also, maximum snow depths were on average but not significantly (t = 1.4; p = 0.204) higher in spring CO_2 burst years (0.89 ± 0.33 m) compared with other years (0.61 ± 0.33 m). The spring CO_2 burst years had significantly (t = 3.0, p = 0.016) weaker CO_2 sink strength (−13.8 ± 7.6 g C m^{-2}) compared with other years (−28.8 ± 9.1 g C m^{-2}; Table 1).

[20] The time period for which the parameterization of the light response curve (equation (1)) was considered significant, that is, when all parameters were significantly different from zero ($p < 0.05$), varied between years. Similar to the net uptake period, the timing when the parameterization became significant in early growing season (DOY 177 ± 8.3) was more variable compared with the timing when the parameterization became insignificant in late growing season (DOY 235 ± 6.1). Mean r^2 and RMSE of the significant light response curve parameterization throughout the whole study period were 0.64 and 0.42, respectively. The rate of CO_2 uptake at light saturation (F_{csat}) followed a bell shaped curve (Figure 4a), where the rates started off slightly below 0.5 μmol m^{-2} s^{-1}, and reached their maximum of 1.95 ± 0.21 μmol m^{-2} s^{-1} at DOY 204 ± 9.2 (23 July). Mean dark respiration, R_d (Figure 4b) and the initial slope of the light response curve, α (Figure 4c) were 1.01 ± 0.23 μmol m^{-2} s^{-1} and 0.011 ± 0.003 μmol μmol^{-1}, respectively, in the end of July (DOY 200–210).

[21] The parameters of the light response curve (equation (1) and Figure 4) were used to model GPP and R_{eco} (Figure 3). Mean daily rates of GPP and R_{eco} throughout the study period were −1.29 ± 0.17 μmol m^{-2} s^{-1} and 0.87 ± 0.15 μmol m^{-2} s^{-1}, respectively, while average maximum daily rates of GPP and R_{eco} were −2.21 ± 0.36 μmol m^{-2} s^{-1} and 1.51 ± 0.23 μmol m^{-2} s^{-1}, respectively. Accumulated NEE (DOY 160–236) and accumulated GPP and R_{eco} (for the time periods of significant parameterization of light response curves) for each year are shown in Table 1 and Figure 5. Mean accumulated NEE was −20.6 ± 11.1 g C m^{-2}, while mean accumulated GPP and R_{eco} were −78.6 ± 13.7 g C m^{-2} and 53.0 ± 10.7 g C m^{-2}, respectively. The coefficient of (interannual) variation was highest for NEE (0.53), followed by R_{eco} (0.20) and GPP (0.18). The estimated total uncertainty for accumulated NEE was on average ± 2.1 g C m^{-2} (approximately ± 10% of accumulated NEE), while for accumulated GPP and R_{eco} the associated uncertainty was estimated to be ± 9.6 g C m^{-2} (±12%) and 9.4 g C m^{-2} (±18%), respectively (Table 1). Of the separate components in the NEE uncertainty analysis (equation (2)), the selection of u_* threshold (E_{ustar}) had highest associated uncertainty (on average ± 1.3 g C m^{-2}), followed by E_{freq}, E_{rand} and E_{gap}. For both accumulated GPP and R_{eco}, highest uncertainty was associated with parameterization of the light response curves (E_{LRC}).

[22] In the first 6 years (2000–2005) of the study period, accumulated GPP became more negative with time (r^2 =

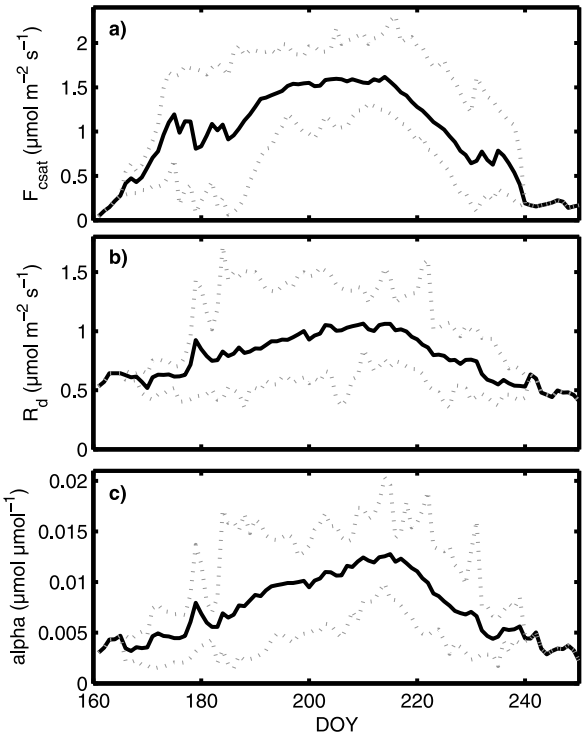

Figure 4. Parameters from the light response curve (equation (1)) used for gap filling and modeling CO_2 flux components: (a) CO_2 uptake at light saturation (F_{csat}), (b) dark respiration (R_d), and (c) initial slope of light response curve (α). Black solid lines depict means, while gray dashed lines depict minimum and maximum values during the study period (2000–2010). The parameterization of the light response curve was considered significant only when all three parameters were significantly different from zero.

0.795, p = 0.017; Figure 5), indicating increased CO_2 assimilation. However, since then the increase leveled off and the GPP sums for 2007–2010 were all in a narrow range of −84 to −88 g C m^{-2}. Ecosystem respiration did also show a close to significant increase in the first 6 years (r^2 = 0.577, p = 0.080). However, in 2003–2006 there was a decline in R_{eco} (r^2 = 0.921, p = 0.040), while in 2006–2009 R_{eco} increased again (r^2 = 0.946, p = 0.027). Accumulated NEE (DOY 160–236) decreased significantly in the years 2001–2005 (r^2 = 0.822, p = 0.034), indicating an increasing CO_2 sink strength during this period. However, after the year 2005 the trend reversed and NEE increased significantly between 2005 and 2010 (r^2 = 0.702, p = 0.037), indicating that the CO_2 sink strength of the Zackenberg heath weakened.

[23] The interannual variation in accumulated NEE, GPP and R_{eco} was mainly explained by variations in midsummer (July) temperature and various temperature-related variables (Table 2). Net ecosystem exchange did not correlate significantly with any ancillary variable, but the relationship with maximum thaw depth was close to significant (p = 0.053). Gross primary production was significantly correlated with maximum thaw depth (p = 0.026), and the relationships to mean July air temperature (p = 0.065) and July growing degree days (p = 0.063) were close to significant. Ecosystem respiration showed significant correlations with mean July air temperature (p = 0.012), July growing degree days (p = 0.013), and maximum thaw depth (p = 0.039).

[24] The CO_2 flux components (NEE, GPP, R_{eco}) did also correlate inherently; there were significant relationships between NEE and GPP (p = 0.039) and GPP and R_{eco} (p = 0.008). However, since R_{eco} is calculated as the difference between NEE and GPP (see section 2), correlation analyses involving R_{eco} and NEE or R_{eco} and GPP will lead to artificial or spurious correlation of the type Y versus $Y + X$ [*Brett*, 2004]. To be able to assess the correlation between

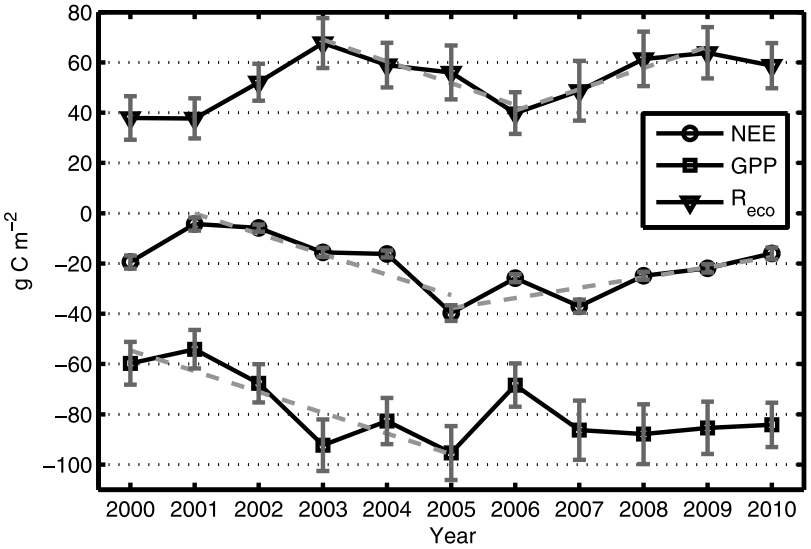

Figure 5. Accumulated CO_2 flux components from the Zackenberg heath, northeast Greenland, 2000–2010. NEE was accumulated for DOY 160–236 (see section 2.4), while GPP and ecosystem respiration (R_{eco}) were accumulated for the time period for which the parameterization of the light response curve was considered significant (see Figure 3). Dashed lines depict periods of significant change in data (see section 3 for r^2 values), while error bars indicate the uncertainty in accumulated values.

Table 2. Accumulated NEE, GPP, and R_{eco} With Associated Uncertainty Estimates, Ancillary Data for Each Year, and Correlation Coefficients[a]

Year	NEE (g C m^{-2})	GPP[b] (g C m^{-2})	R_{eco} (g C m^{-2})	SM DOY	Max Thaw (cm)	AirT July (°C)	Precip July[c] (mm)	GDD July	PPFD July (μmol m^{-2} s^{-1})	NDVI	VPD July (kPa)
2000	−19.4 ± 2.6	−59.7 ± 8.5	37.9 ± 8.7	166	61.6	5.3	13	164	459	0.57	0.27
2001	−4.3 ± 2.6	−54.1 ± 7.7	37.7 ± 8.0	175	61.5	4.9	7	152	466	0.46	0.25
2002	−5.9 ± 1.4	−67.7 ± 7.6	52.1 ± 7.3	171	65.1	5.7	11	176	424	0.52	0.14
2003	−15.6 ± 1.8	−92.3 ± 10.2	67.7 ± 9.9	165	68.0	7.7	6	237	431	-	0.29
2004	−16.2 ± 1.4	−82.7 ± 9.2	58.9 ± 8.9	165	70.7	7.2	10	222	463	-	0.30
2005	−39.7 ± 3.1	−95.4 ± 10.7	56.0 ± 10.7	158	74.0	6.9	28	215	427	0.44	0.31
2006	−25.8 ± 1.6	−68.4 ± 8.6	39.8 ± 8.3	182	71.8	6.6	12	205	518	-	0.28
2007	−37.0 ± 2.6	−86.3 ± 11.8	48.7 ± 11.9	159	71.0	5.9	8	182	530	0.50	0.24
2008	−24.9 ± 1.6	−87.9 ± 11.9	61.4 ± 10.8	176	73.5	8.7	8	271	547	0.51	0.37
2009	−21.9 ± 1.7	−85.4 ± 10.4	63.8 ± 10.2	136	76.2	8.6	26	266	483	0.46	0.36
2010	−16.0 ± 2.3	−84.2 ± 8.8	58.7 ± 9.0	167	73.9	5.3	1	166	529	0.53	0.20

Correlation Coefficients	NEE	GPP[b]	R_{eco}	SM DOY	Max Thaw	AirT July	Precip July[c]	GDD July	PPFD July	NDVI	VPD July
NEE	1	0.63[d]	−0.10	0.29	−0.60	−0.31	−0.35	−0.32	−0.30	0.28	−0.43
GPP		1	−0.75[e,f]	0.42	−0.66[d]	−0.57	−0.12	−0.58	−0.08	0.50	−0.43
R_{eco}			1	−0.47	0.63[d]	0.72[d]	0.10	0.72[d]	−0.05	−0.29	0.34

[a]SM DOY, snowmelt DOY; Max Thaw, maximum thaw depth; AirT July, mean July air temperature; Precip July, July precipitation sum; GDD July, July growing degree days; PPFD July, mean July photosynthetic photon flux density; NDVI, normalized difference vegetation index; VPD July, mean July vapor pressure deficit.
[b]Transformed log(x + 100).
[c]Transformed log(x).
[d]Correlation is significant at the $\alpha = 0.05$ level.
[e]$\alpha = 0.01$ level.
[f]$p = 0.742 \pm 0.014$ after accounting for the spurious correlation emanating from the derivation of R_{eco} from the difference between NEE and GPP [*Brett*, 2004].

GPP and R_{eco} independent of the flux partitioning method, we used a bootstrap simulation methodology described by *Brett* [2004] and *Lund et al.* [2010]. This procedure showed that after accounting for the spurious correlation introduced by the flux partitioning procedure the relationship between GPP and R_{eco} was no longer significant ($p = 0.742 \pm 0.014$). Neither are the variables NEE and GPP entirely independent, since NEE is used to estimate the parameters for modeling GPP. Thus, the significance between NEE and GPP may be overestimated and should be interpreted with caution.

[25] The fit between accumulated GPP and mean July air temperature was improved when using a second-order polynomial fit compared with a first-order, since the increase in GPP rates leveled off at the high end of observed temperature range (Figure 6b). The adjusted r^2 value (using log (x + 100) transformed GPP data) increased from 0.24 (first order) to 0.29 (second order). For the significant relationship between R_{eco} and mean July air temperature the adjusted r^2 value decreased from 0.47 to 0.40 for first- and second-order polynomials, respectively (Figure 6c). As R_{eco} generally responds exponentially to temperature, the well-known *Lloyd and Taylor* [1994] equation was also evaluated, resulting in an adjusted r^2 value of 0.51. The correlation between NEE and mean July air temperature was not significant (Table 2), but there was a trend toward increasing sink strength with increasing temperature. However, highest CO_2 accumulation did not occur in the warmest years, rather in years with average temperature (Figure 6a).

4. Discussion

[26] The footprint analysis revealed that a majority of the measured CO_2 fluxes emanated from the *Cassiope* heath plant community type (Figure 1). The dominating plant species, *Cassiope tetragona* and *Salix arctica* are common species in Greenland (covering approximately 31% of the Zackenberg valley [*Soegaard et al.*, 2000]) and occur throughout most of the circumpolar middle and high Arctic areas. In the Circumpolar Arctic Vegetation Mapping project [*Circumpolar Arctic Vegetation Mapping Team*, 2003] this type is classified as "prostrate/hemiprostrate dwarf-shrub tundra" and covers approximately 140.000 km^2 of the Arctic, corresponding to 10% of the high and middle Arctic area (Bioclimate Subzones A–C).

[27] Flux measurements from comparable sites are scarce. Most Arctic CO_2 flux data exist for wet ecosystems, which have larger rates of NEE, GPP and R_{eco} [*Soegaard and Nordstroem*, 1999; *Vourlitis and Oechel*, 1999; *Vourlitis et al.*, 2000; *Nordstroem et al.*, 2001; *Harazono et al.*, 2003; *Aurela et al.*, 2004; *Corradi et al.*, 2005; *Johansson et al.*, 2006; *Kutzbach et al.*, 2007; *Lafleur and Humphreys*, 2008; *Parmentier et al.*, 2011], likely because wetter conditions allow for higher biomass and LAI, factors that are known to regulate CO_2 fluxes [*McFadden et al.*, 2003; *Lund et al.*, 2010]. *McFadden et al.* [2003] studied a wide range of ecosystems in northern Alaska, including two heath sites that were slightly drier (mean soil water content 16%) and had thicker active layers (>1 m) compared with the Zackenberg heath. Their growing season mean NEE was ca. −0.6 to −0.7 g C m^{-2} d^{-1}, which is similar to mean daily NEE in July in this study (−0.58 ± 0.17 g C m^{-2} d^{-1}). The mid-season mean NEE (31 July to 11 August) in a high Arctic polar semi desert site on Svalbard [*Lloyd*, 2001] was, however, lower than in the Zackenberg heath, amounting to −0.19 g C m^{-2} d^{-1}. *Humphreys and Lafleur* [2011] studied

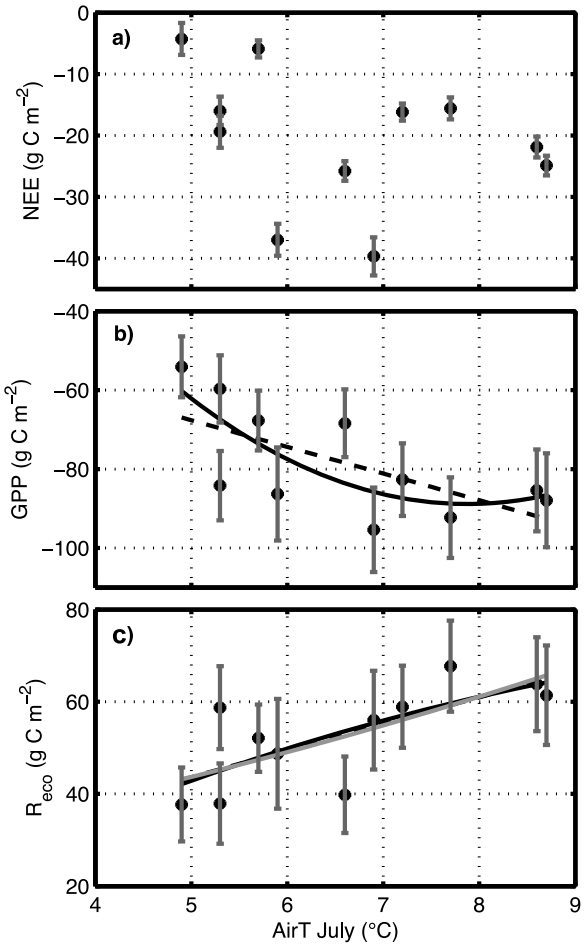

Figure 6. Scatterplots of CO_2 flux components versus mean July air temperatures (AirT July). (a) Accumulated NEE. (b) GPP. Here, the untransformed GPP values are shown to ease the visualization and interpretation. (c) Ecosystem respiration (R_{eco}). Black dots depict first-order polynomial fits, black solid lines depict second-order polynomial fits, and gray solid line (in Figure 6c) is the *Lloyd and Taylor* [1994] relationship (see section 3 for r^2 values).

a Canadian mixed tundra site that had higher rates of midseason NEE (ca. -1.0 g C m^{-2} d^{-1}), possibly related to higher LAI at their site (0.70 ± 0.21) compared with the Zackenberg tundra heath.

[28] The seasonal evolution of the light response curve parameters (F_{csat}, R_d, α) time series (Figure 4) followed a bell shaped curve, indicating a relationship to plant development and LAI over the growing season. The dynamics were similar to a study on four north European mires [*Lindroth et al.*, 2007]; however, the absolute values were lower in the present study owing to colder conditions. The most comparable site in the work of *Lindroth et al.* [2007], the subarctic fen Kaamanen, had peak values of F_{csat}, R_d, and α amounting to 4.5 μmol m^{-2} s^{-1}, 1.8 μmol m^{-2} s^{-1}, and 0.023 μmol μmol^{-1}, respectively. These differences are also reflected by differences in flux rates between Kaamanen and the Zackenberg heath. *Lloyd* [2001] used a different light response curve; however, their P_{max} (maximum rate of photosynthesis) can be compared with $F_{csat} + R_d$ in this study. Midseason P_{max} for the high Arctic polar semi desert site was 1.8 μmol m^{-2} s^{-1}, as compared with 2.3 ± 0.33 μmol m^{-2} s^{-1} ($F_{csat} + R_d$) for the Zackenberg heath in the same period.

[29] The timing of start of period with mean daily net CO_2 uptake was more variable than the timing of end of uptake period. This was related to timing of snowmelt; a snowpack limits light penetration to vegetation and therefore minimizes photosynthetic assimilation of atmospheric CO_2. The end of the net CO_2 uptake period is more related to fading light conditions due to the high-latitude location of the study site (74.47°N). Future changes in the length of the mean daily net CO_2 uptake period will thus be controlled by changes in wintertime precipitation and springtime temperature, regulating the timing of snow cover melt. If a changing climate brings about earlier springtime snowmelt, plants may respond immediately and begin assimilating CO_2, while changes in temperature and snow conditions during autumn would have comparably low effects on the CO_2 dynamics owing to the low amount of solar radiation. The noticeable prevalence of increased CO_2 emissions between snowmelt period and start of daily net CO_2 uptake period in some years, the spring CO_2 burst years (2001–2004, 2008, and 2010), constituted an interesting feature of the Zackenberg heath. The occurrence of these episodic emissions was related to soil temperatures and snow dynamics. Years with spring CO_2 burst had preceding winters with deep and long-lasting snowpacks. Below a thick snowpack soils will be insulated from reaching low temperatures; and at the same time the snowpack will act as a lid by increasing diffusive resistance, preventing respired CO_2 from being transported to the atmosphere [*McDowell et al.*, 2000]. When snowmelt begins in spring, CO_2 stored in soil and snow cavities will be released and the comparably high soil temperatures will maintain reasonable respiration rates. It can be noticed that the spring CO_2 burst years had lower CO_2 sink strengths compared with the other years (Table 1). Earlier studies have found that the date of snowmelt and length of snow-free period are important for the annual CO_2 balance, in the sense that it regulates length of growing season period [*Aurela et al.*, 2004; *Grøndahl et al.*, 2007]. Our results show that snowpack depth and duration are primarily important for CO_2 budgets through the effect on winter and spring respiration, which is in line with previous studies [*Welker et al.*, 2000; *Bubier et al.*, 2002; *Monson et al.*, 2006; *Nobrega and Grogan*, 2007; *Nowinski et al.*, 2010; *Humphreys and Lafleur*, 2011]. However, as the CO_2 budgets in this study (Table 1) are calculated for a limited period of the year (DOY 160–236), which includes most of the increased emission episodes (Figure 3); it cannot be excluded that accumulated wintertime CO_2 emissions are higher for years without the spring CO_2 burst which could partly offset the effect on the annual budget. Year-round measurements are required to further investigate this phenomenon. *Welker et al.* [2000] found that increased wintertime CO_2 efflux resulted in reduced summer time emissions. In this study, accumulated R_{eco} (not including the spring CO_2 burst) were on average (insignificantly) higher for spring CO_2 burst years (56.1 g C m^{-2}) compared with other years (49.2 g C m^{-2}), suggesting that the increased spring CO_2 emissions did not exhaust the labile soil C pool and that respiration rates were not reduced during the summer period.

[30] The increase in accumulated GPP as a response to increased July air temperature leveled off at the high end of the observed temperature range (Figure 6). Thus, plant CO_2 assimilation did not benefit further from additional summertime warming. Other environmental characteristics may act to limit GPP in warm summers, such as plant water or nutrient availability. The effect of soil water content on the CO_2 exchange could not be evaluated on the whole data set because continuous data are only available from the heath ecosystem since late 2005. For the 2 years with highest July temperatures, 2008 and 2009, the mean July soil water content in top 10 cm was 29.6% and 29.3%, respectively. For the same period in 2006 and 2007, the mean soil water content was 33.9% and 27.2%, respectively, indicating that 2008 and 2009 were not exceptionally dry. However, July vapor pressure deficit (VPD) was higher in 2008 and 2009 compared with other years, indicating that plant water stress increasing stomatal resistance and thus limiting photosynthesis could be an explanation as to why GPP was not higher in 2008 and 2009 despite higher summertime temperatures. Another important factor for GPP is N availability, which has been found to be limiting plant growth in various plant community types in Zackenberg [*Arndal et al.*, 2009]. It is possible that the deviation from the linear relationship between accumulated GPP and July air temperature can be partly related to N deficiency. As mineralization rates are expected to increase as a response to climate warming, more N will become available [*Rustad et al.*, 2001]; however, the vegetation nutritional demands may increase at an even higher rate.

[31] In a land surface phenology study using spectral measures in the Zackenberg area, *Tamstorf et al.* [2007] found a nonlinear response of seasonally integrated NDVI to temperature in the *Cassiope* heath, where NDVI increased with increasing temperature to a certain point and then decreased. Their explanation for this phenomenon was a limitation of plant photosynthesis due to enzymatic inhibition of the photosynthetic apparatus. Some recent studies have documented thermal adaptation of NEE, GPP and R_{eco} across a broad range of thermal gradients [*Baldocchi et al.*, 2001; *Atkin and Tjoelker*, 2003; *Gunderson et al.*, 2010; *Yuan et al.*, 2011]. *Baldocchi et al.* [2001] suggested that the thermal optimum for ecosystem-scale GPP is a function of mean summer temperature. Our study suggests that a mean July temperature of approximately 7°C represents the temperature optimum for GPP in an Arctic tundra heath, while 6°C–7°C appears to be optimal for NEE (Figure 6). These values are close to the long-term (1996–2010) average of mean July temperature (6.2°C). A recent study [*Yuan et al.*, 2011] has also demonstrated that ecosystem NEE adapts to temperature as they found that maximum CO_2 uptake across a wide range of ecosystems was strongly correlated with mean temperature during the period of net CO_2 uptake. *Soegaard and Nordstroem* [1999] combined CO_2 fluxes measured by an eddy covariance system in a sedge-dominated fen in Zackenberg with a photosynthesis model [*Collatz et al.*, 1991] and a soil respiration model. They found that the fen ecosystem was functioning close to optimally in terms of CO_2 sink capacity given the actual temperature conditions. An increase (or decrease) in temperature was predicted to reduce the ecosystem CO_2 assimilation. Even though *Soegaard and Nordstroem* [1999] studied a different ecosystem type (fen) compared with the present study (heath), it can be argued that the inherent thermal optimality dynamics in various ecosystems in the area is similar since they are subjected to the same meteorological conditions. Our results show that the CO_2 sink strength of the Zackenberg heath was weaker in the two warmest years compared with years with temperatures close to the long-term average, possibly suggesting that climate warming in this high-latitude area is more rapid than what the ecosystem can adapt to. Although plant species have the ability to adapt and acclimate to increased temperatures [*Gunderson et al.*, 2010], such dynamics are likely to vary between species and ecosystems. In areas subjected to strong warming, such as the Arctic, the rate of warming may exceed the rate of plant adaptation. If this hypothesis holds and can be applied to other ecosystems, it will have implications for our current understanding of ecosystems dynamics as well as the response of the terrestrial carbon cycle to global warming.

[32] If the strong summertime warming continues in the Zackenberg area, our results indicate that the tundra heath CO_2 sink strength will weaken. Eventually, the site may even turn into a C source. Similar conclusions were drawn by *Parmentier et al.* [2011], who found that years with low accumulated CO_2 uptake in a Siberian graminoid tundra site had long growing seasons or high summer temperatures. However, future CO_2 exchange is dependent on possible changes in vegetation structure and composition as a response to a changing climate. The large expansion of shrubs observed in large areas across the Arctic [*Sturm et al.*, 2001; *Tape et al.*, 2006] has not been observed at this site (N. M. Schmidt, manuscript in preparation, 2012); however, global warming will inevitably affect Arctic ecosystems structure and functioning with associated effects on the C cycling.

5. Conclusions

[33] This study summarizes more than a decade (2000–2010) of eddy covariance measurements of the land-atmosphere CO_2 exchange in a high Arctic tundra heath site in northeast Greenland (Zackenberg). Snow cover depth and duration were found to affect both springtime CO_2 fluxes and timing of start of period with mean daily CO_2 uptake. In the first part of the study period, there was a significant increase in gross primary production (GPP) and CO_2 sink strength of approximately 8 g C m^{-2} yr^{-1}. In the last few years there were no changes in GPP; instead ecosystem respiration (R_{eco}) increased significantly (8.5 g C m^{-2} yr^{-1}) and the CO_2 sink strength weakened (-4.1 g C m^{-2} yr^{-1}). A linear correlation analysis revealed that July air temperature, growing degree days and maximum thaw depth regulated the interannual variation in accumulated sums of net ecosystem exchange, GPP and R_{eco}. However, the increase in accumulated GPP leveled off at the high end of the observed temperature range, suggesting that a continued warming will not increase GPP, and that the CO_2 sink strength of the Zackenberg heath will weaken.

[34] **Acknowledgments.** The authors wish to thank the GeoBasis program for running the eddy covariance systems and Zackenberg Ecological Research Operations for logistical support.

References

Arndal, M. F., L. Illeris, A. Michelsen, K. Albert, M. Tamstorf, and B. U. Hansen (2009), Seasonal variation in gross ecosystem production, plant biomass, and carbon and nitrogen pools in five high arctic vegetation types, *Arct. Antarct. Alp. Res.*, *41*(2), 164–173, doi:10.1657/1938-4246-41.2.164.

Atkin, O. K., and M. G. Tjoelker (2003), Thermal acclimation and the dynamic response of plant respiration to temperature, *Trends Plant Sci.*, *8*(7), 343–351, doi:10.1016/S1360-1385(03)00136-5.

Aurela, M., T. Laurila, and J.-P. Tuovinen (2002), Annual CO_2 balance of a subarctic fen in northern Europe: Importance of the wintertime efflux, *J. Geophys. Res.*, *107*(D21), 4607, doi:10.1029/2002JD002055.

Aurela, M., T. Laurila, and J.-P. Tuovinen (2004), The timing of snow melt controls the annual CO_2 balance in a subarctic fen, *Geophys. Res. Lett.*, *31*, L16119, doi:10.1029/2004GL020315.

Aurela, M., T. Riutta, T. Laurila, J.-P. Tuovinen, T. Vesala, E.-S. Tuittila, J. Rinne, S. Haapanala, and J. Laine (2007), CO_2 exchange of a sedge fen in southern Finland: The impact of a drought period, *Tellus, Ser. B*, *59*, 826–837, doi:10.1111/j.1600-0889.2007.00309.x.

Baldocchi, D. D. (2003), Assessing the eddy covariance technique for evaluating carbon dioxide exchange rates of ecosystems: Past, present and future, *Global Change Biol.*, *9*(4), 479–492, doi:10.1046/j.1365-2486.2003.00629.x.

Baldocchi, D. D., et al. (2001), FLUXNET: A new tool to study the temporal and spatial variability of ecosystem-scale carbon dioxide, water vapor, and energy flux densities, *Bull. Am. Meteorol. Soc.*, *82*(11), 2415–2434, doi:10.1175/1520-0477(2001)082<2415:FANTTS>2.3.CO;2.

Brett, M. T. (2004), When is a correlation between non-independent variables 'spurious'?, *Oikos*, *105*(3), 647–656, doi:10.1111/j.0030-1299.2004.12777.x.

Bubier, J. L., P. Crill, and A. Mosedale (2002), Net ecosystem CO_2 exchange measured by autochambers during the snow-covered season at a temperate peatland, *Hydrol. Processes*, *16*(18), 3667–3682, doi:10.1002/hyp.1233.

Circumpolar Arctic Vegetation Mapping Team (2003), Circumpolar Arctic Vegetation Map, *CAFF Map 1*, scale 1:7,500,000, U.S. Fish and Wildlife Serv., Anchorage, Alaska.

Collatz, G. J., J. T. Ball, C. Grivet, and J. A. Berry (1991), Physiological and environmental regulation of stomatal conductance, photosynthesis and transpiration: A model that includes a laminar boundary layer, *Agric. For. Meteorol.*, *54*, 107–136, doi:10.1016/0168-1923(91)90002-8.

Corradi, C., O. Kolle, K. M. Walter, S. A. Zimov, and E.-D. Schulze (2005), Carbon dioxide and methane exchange of a north-east Siberian tussock tundra, *Global Change Biol.*, *11*(11), 1910–1925, doi:10.1111/j.1365-2486.2005.01023.x.

Dorrepaal, E., S. Toet, R. S. P. van Logtestijn, E. Swart, M. J. van de Weg, T. V. Callaghan, and R. Aerts (2009), Carbon respiration from subsurface peat accelerated by climate warming in the subarctic, *Nature*, *460*, 616–619, doi:10.1038/nature08216.

Elberling, B., M. P. Tamstorf, and A. Michelsen (2008), Soil and plant community characteristics and dynamics at Zackenberg, *Adv. Ecol. Res.*, *40*, 223–248, doi:10.1016/S0065-2504(07)00010-4.

Elbers, J. A., C. M. J. Jacobs, B. Kruijt, W. W. P. Jans, and E. J. Moors (2011), Assessing the uncertainty of estimated annual totals of net ecosystem productivity: A practical approach applied to a mid latitude temperate pine forest, *Agric. For. Meteorol.*, *151*, 1823–1830, doi:10.1016/j.agrformet.2011.07.020.

Falge, E., et al. (2001), Gap filling strategies for defensible annual sums of net ecosystem exchange, *Agric. For. Meteorol.*, *107*, 43–69, doi:10.1016/S0168-1923(00)00225-2.

Graversen, R. G., T. Mauritsen, M. Tjernström, E. Källén, and G. Svensson (2008), Vertical structure of recent Arctic warming, *Nature*, *451*, 53–56, doi:10.1038/nature06502.

Grøndahl, L., T. Friborg, and H. Soegaard (2007), Temperature and snow-melt controls on interannual variability in carbon exchange in the high Arctic, *Theor. Appl. Climatol.*, *88*, 111–125, doi:10.1007/s00704-005-0228-y.

Grøndahl, L., T. Friborg, T. R. Christensen, A. Ekberg, B. Elberling, L. Illeris, C. Nordstroem, Å. Rennermalm, C. Sigsgaard, and H. Soegaard (2008), Spatial and inter-annual variability of trace gas fluxes in a heterogeneous high-arctic landscape, *Adv. Ecol. Res.*, *40*, 473–498, doi:10.1016/S0065-2504(07)00020-7.

Gunderson, C. A., K. H. O'Hara, C. M. Campion, A. V. Walker, and N. T. Edwards (2010), Thermal plasticity of photosynthesis: The role of acclimation in forest responses to a warming climate, *Global Change Biol.*, *16*(8), 2272–2286, doi:10.1111/j.1365-2486.2009.02090.x.

Hansen, B. U., C. Sigsgaard, L. Rasmussen, J. Cappelen, J. Hinkler, S. H. Mernild, D. Petersen, M. P. Tamstorf, M. Rasch, and B. Hansholt (2008), Present-day climate at Zackenberg, *Adv. Ecol. Res.*, *40*, 111–149, doi:10.1016/S0065-2504(07)00006-2.

Harazono, Y., M. Mano, A. Miyata, R. C. Zulueta, and W. C. Oechel (2003), Inter-annual carbon dioxide uptake of a wet sedge tundra ecosystem in the Arctic, *Tellus, Ser. B*, *55*, 215–231, doi:10.1034/j.1600-0889.2003.00012.x.

Højstrup, J. (1993), A statistical data screening procedure, *Meas. Sci. Technol.*, *4*, 153–157, doi:10.1088/0957-0233/4/2/003.

Humphreys, E. R., and P. M. Lafleur (2011), Does earlier snowmelt lead to greater CO_2 sequestration in two low Arctic tundra ecosystems?, *Geophys. Res. Lett.*, *38*, L09703, doi:10.1029/2011GL047339.

Jensen, L. M., and M. Rasch (2010), *Zackenberg Ecological Research Operations: 15th Annual Report, 2009*, Natl. Environ. Res. Inst., Aarhus Univ., Roskilde, Denmark.

Johansson, T., N. Malmer, P. M. Crill, T. Friborg, J. H. Åkerman, M. Mastepanov, and T. R. Christensen (2006), Decadal vegetation changes in a northern peatland, greenhouse gas fluxes and net radiative forcing, *Global Change Biol.*, *12*(12), 2352–2369, doi:10.1111/j.1365-2486.2006.01267.x.

Kutzbach, L., C. Wille, and E.-M. Pfeiffer (2007), The exchange of carbon dioxide between wet arctic tundra and the atmosphere at the Lena River Delta, Northern Siberia, *Biogeosciences*, *4*(5), 869–890, doi:10.5194/bg-4-869-2007.

Lafleur, P. M., and E. R. Humphreys (2008), Spring warming and carbon dioxide exchange over low Arctic tundra in central Canada, *Global Change Biol.*, *14*(4), 740–756, doi:10.1111/j.1365-2486.2007.01529.x.

Lindroth, A., et al. (2007), Environmental controls on the CO_2 exchange in north European mires, *Tellus, Ser. B*, *59*, 812–825, doi:10.1111/j.1600-0889.2007.00310.x.

Lloyd, C. R. (2001), On the physical controls of the carbon dioxide balance at a high Arctic site in Svalbard, *Theor. Appl. Climatol.*, *70*, 167–182, doi:10.1007/s007040170013.

Lloyd, J., and J. A. Taylor (1994), On the temperature dependence of soil respiration, *Funct. Ecol.*, *8*(3), 315–323, doi:10.2307/2389824.

Lund, M., A. Lindroth, T. R. Christensen, and L. Ström (2007), Annual CO_2 balance of a temperate bog, *Tellus, Ser. B*, *59*, 804–811, doi:10.1111/j.1600-0889.2007.00303.x.

Lund, M., et al. (2010), Variability in exchange of CO_2 across 12 northern peatland and tundra sites, *Global Change Biol.*, *16*(9), 2436–2448, doi:10.1111/j.1365-2486.2009.02104.x.

Mack, M. C., E. A. G. Schuur, M. S. Bret-Harte, G. R. Shaver, and F. S. Chapin (2004), Ecosystem carbon storage in arctic tundra reduced by long-term nutrient fertilization, *Nature*, *431*, 440–443, doi:10.1038/nature02887.

Malmer, N., and B. Wallén (2005), Nitrogen and phosphorus in mire plants: Variation during 50 years in relation to supply rate and vegetation type, *Oikos*, *109*(3), 539–554, doi:10.1111/j.0030-1299.2001.13835.x.

McDowell, N. G., J. D. Marshall, T. D. Hooker, and R. Musselman (2000), Estimating CO_2 flux from snowpacks at three sites in the Rocky Mountains, *Tree Physiol.*, *20*, 745–753.

McFadden, J. P., W. Eugster, and F. S. Chapin (2003), A regional study of the controls on water vapor and CO_2 exchange in Arctic tundra, *Ecology*, *84*(10), 2762–2776, doi:10.1890/01-0444.

McGuire, A. D., et al. (2009), Sensitivity of the carbon cycle in the Arctic to climate change, *Ecol. Monogr.*, *79*(4), 523–555, doi:10.1890/08-2025.1.

McGuire, A. D., R. W. MacDonald, E. A. G. Schuur, J. W. Harden, P. Kuhry, D. J. Hayes, T. R. Christensen, and M. Heimann (2010), The carbon budget of the northern cryosphere region, *Curr. Opin. Environ. Sustainability*, *2*, 231–236, doi:10.1016/j.cosust.2010.05.003.

Moncrieff, J. B., J. M. Massheder, H. de Bruin, J. Elbers, T. Friborg, B. Heusinkveld, P. Kabat, S. Scott, H. Soegaard, and A. Verhoef (1997), A system to measure surface fluxes of momentum, sensible heat, water vapor and carbon dioxide, *J. Hydrol.*, *188–189*, 589–611, doi:10.1016/S0022-1694(96)03194-0.

Monson, R. K., D. L. Lipson, S. P. Burns, A. A. Turnipseed, A. C. Delany, M. W. Williams, and S. K. Schmidt (2006), Winter forest soil respiration controlled by climate and microbial community composition, *Nature*, *439*, 711–714, doi:10.1038/nature04555.

Moore, C. J. (1986), Frequency response corrections for eddy correlation systems, *Boundary Layer Meteorol.*, *37*(1–2), 17–35, doi:10.1007/BF00122754.

Nobrega, S., and P. Grogan (2007), Deeper snow enhances winter respiration from both plant-associated and bulk soil carbon pools in birch hummock tundra, *Ecosystems*, *10*, 419–431, doi:10.1007/s10021-007-9033-z.

Nordstroem, C., H. Soegaard, T. R. Christensen, T. Friborg, and B. U. Hansen (2001), Seasonal carbon dioxide balance and respiration of a high-arctic fen ecosystem in NE-Greenland, *Theor. Appl. Climatol.*, *70*, 149–166, doi:10.1007/s007040170012.

Nowinski, N. S., L. Taneva, S. E. Trumbore, and J. M. Welker (2010), Decomposition of old organic matter as a result of deeper active layers in a snow depth manipulation experiment, *Oecologia*, *163*, 785–792, doi:10.1007/s00442-009-1556-x.

Oechel, W. C., S. J. Hastings, G. L. Vourlitis, M. Jenkins, G. Riechers, and N. Grulke (1993), Recent change of arctic tundra ecosystems from a net carbon dioxide sink to a source, *Nature*, *361*, 520–523, doi:10.1038/361520a0.

Parmentier, F. J. W., M. K. van der Molen, J. van Huissteden, S. A. Karsanaev, A. V. Kononov, D. A. Suzdalov, T. C. Maximov, and A. J. Dolman (2011), Longer growing seasons do not increase net carbon uptake in the northeastern Siberian tundra, *J. Geophys. Res.*, *116*, G04013, doi:10.1029/2011JG001653.

Romanovsky, V. E., et al. (2010), Thermal state of permafrost in Russia, *Permafrost Periglacial Processes*, *21*, 136–155, doi:10.1002/ppp.683.

Rustad, L. E., J. L. Campbell, G. M. Marion, R. J. Norby, M. J. Mitchell, A. E. Hartley, J. H. C. Cornelissen, J. Gurevitch, and GCTE-NEWS (2001), A meta-analysis of the response of soil respiration, net nitrogen mineralization, and aboveground plant growth to experimental ecosystem warming, *Oecologia*, *126*, 543–562, doi:10.1007/s004420000544.

Schuepp, P. H., M. Y. Leclerc, J. I. MacPherson, and R. L. Desjardins (1990), Footprint prediction of scalar fluxes from analytical solutions of the diffusion equation, *Boundary Layer Meteorol.*, *50*(1–4), 355–373, doi:10.1007/BF00120530.

Schuur, E. A. G., et al. (2008), Vulnerability of permafrost carbon to climate change: Implications for the global carbon cycle, *BioScience*, *58*(8), 701–714, doi:10.1641/B580807.

Schuur, E. A. G., J. G. Vogel, K. G. Crummer, H. Lee, J. O. Sickman, and T. E. Osterkamp (2009), The effect of permafrost thaw on old carbon release and net carbon exchange from tundra, *Nature*, *459*, 556–559, doi:10.1038/nature08031.

Soegaard, H., and C. Nordstroem (1999), Carbon dioxide exchange in a high-arctic fen estimated by eddy covariance measurements and modeling, *Global Change Biol.*, *5*(5), 547–562, doi:10.1046/j.1365-2486.1999.00250.x.

Soegaard, H., C. Nordstroem, T. Friborg, B. U. Hansen, T. R. Christensen, and C. Bay (2000), Trace gas exchange in a high-arctic valley: 3. Integrating and scaling CO_2 fluxes from canopy to landscape using flux data, footprint modeling and remote sensing, *Global Biogeochem. Cycles*, *14*(3), 725–744, doi:10.1029/1999GB001137.

Soegaard, H., N. O. Jensen, E. Bøgh, C. B. Hasager, K. Schelde, and A. Thomsen (2003), Carbon dioxide exchange over agricultural landscape using eddy correlation and footprint modeling, *Agric. For. Meteorol.*, *114*, 153–173, doi:10.1016/S0168-1923(02)00177-6.

Sturm, M., C. Racine, and K. Tape (2001), Climate change: Increasing shrub abundance in the Arctic, *Nature*, *411*, 546–547, doi:10.1038/35079180.

Tamstorf, M. P., L. Illeris, B. U. Hansen, and M. Wisz (2007), Spectral measures and mixed models as valuable tools for investigating controls on land surface phenology in high arctic Greenland, *BMC Ecol.*, *7*(9), 1–16, doi:10.1186/1472-6785-7-9.

Tape, K., M. Sturm, and C. Racine (2006), The evidence for shrub expansion in northern Alaska and the Pan-Arctic, *Global Change Biol.*, *12*(4), 686–702, doi:10.1111/j.1365-2486.2006.01128.x.

Tarnocai, C., J. G. Canadell, E. A. G. Schuur, P. Kuhry, G. Mazhitova, and S. A. Zimov (2009), Soil organic carbon pools in the northern circumpolar permafrost region, *Global Biogeochem. Cycles*, *23*, GB2023, doi:10.1029/2008GB003327.

Vourlitis, G. L., and W. C. Oechel (1999), Eddy covariance measurements of CO_2 and energy fluxes of an Alaskan tussock tundra ecosystem, *Ecology*, *80*, 686–701, doi:10.1890/0012-9658(1999)080[0686:ECMOCA]2.0.CO;2.

Vourlitis, G. L., Y. Harazono, W. C. Oechel, M. Yoshomito, and M. Mano (2000), Spatial and temporal variations in hectare-scale net CO_2 flux, respiration and gross primary production of Arctic tundra ecosystems, *Funct. Ecol.*, *14*, 203–214, doi:10.1046/j.1365-2435.2000.00419.x.

Wang, T., et al. (2011), Controls on winter ecosystem respiration in temperate and boreal ecosystems, *Biogeosciences*, *8*(7), 2009–2025, doi:10.5194/bg-8-2009-2011.

Webb, E. K., G. I. Pearman, and R. Leuning (1980), Correction of flux measurements for density effects due to heat and water vapor transfer, *Q. J. R. Meteorol. Soc.*, *106*, 85–100, doi:10.1002/qj.49710644707.

Welker, J. M., J. T. Fahnestock, and M. H. Jones (2000), Annual CO_2 flux in dry and moist Arctic tundra: Field responses to increases in summer temperatures and winter snow depth, *Clim. Change*, *44*, 139–150, doi:10.1023/A:1005555012742.

Yuan, W., et al. (2011), Thermal adaptation of net ecosystem exchange, *Biogeosciences*, *8*(6), 1453–1463, doi:10.5194/bg-8-1453-2011.

J. M. Falk, Department of Earth and Ecosystem Sciences, Lund University, Sölvegatan 12, SE-22362 Lund, Sweden.

T. Friborg and H. Soegaard, Department of Geography and Geology, University of Copenhagen, Øster Voldgade 10, DK-1350 Copenhagen, Denmark.

M. Lund, H. N. Mbufong, C. Sigsgaard, and M. P. Tamstorf, Department of Bioscience, Aarhus University, Frederiksborgvej 399, DK-4000 Roskilde, Denmark. (ml@dmu.dk)